Thermal expansion

11

When a material is heated uniformly it undergoes a strain described by the relationship

$$x_{ij} = \alpha_{ij} \Delta T,$$

where α_{ij} are the thermal expansion coefficients and ΔT is the change in temperature. Room temperature thermal expansion coefficients range from about 10^{-6}/K for an oxide like silica glass to 10^{-3}/K for an elastomeric polymer. Thermal expansion coefficients are often a strong function of temperature, as shown in Fig. 11.1. Simple linear relations are insufficient to describe thermal expansion over a wide temperature range. A power series consisting of terms in ΔT, $(\Delta T)^2$ and higher order terms can be used to describe this thermal expansion over extended temperature ranges. In hexagonal zinc oxide both coefficients are slightly negative at low temperatures and exhibit increasing anisotropy at high temperatures. The negative thermal expansion coefficients are attributed to the low-energy transverse vibrations that dominate at very low temperatures.

11.1 Effect of symmetry

Thermal expansion relates a second rank tensor (strain) to a scalar (temperature change). It is a symmetric second rank tensor because the strain tensor

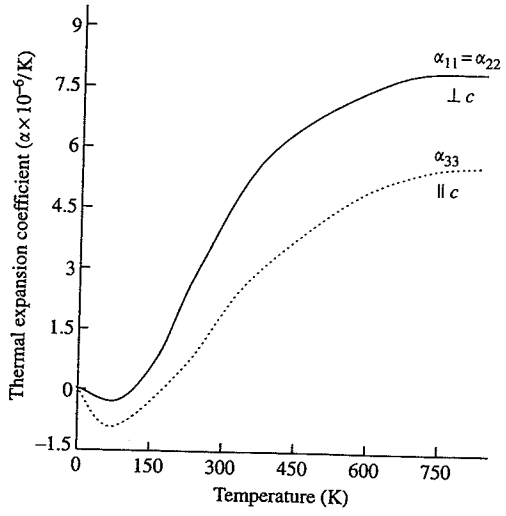

Fig. 11.1 Zinc oxide is a hexagonal crystal with tetrahedrally bonded zinc and oxygen atoms. The thermal expansion coefficients approach zero at 0 K. Anisotropy also changes sign at low temperatures with both coefficients becoming slightly negative.

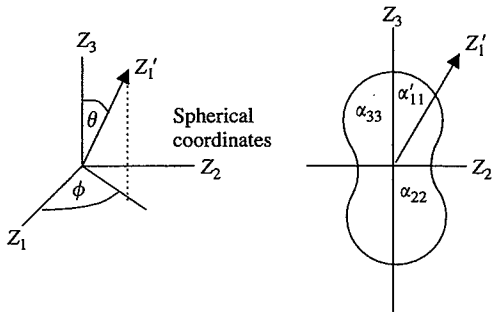

Fig. 11.2 Anisotropy surface for the thermal expansion coefficient of low symmetry crystals.

is symmetric. Therefore thermal expansion and the dielectric constant are the same type of tensor, and the effect of symmetry is the same. This means that for the general case (a triclinic crystal), six measurements are required to find the three principal thermal expansion coefficients and the three angles needed to orient the principal axes. The appropriate matrices for other symmetries are given in Table 9.1. Four measurements are needed for monoclinic crystals, three for orthorhombic, two for trigonal, tetragonal, and hexagonal crystals, and only one for cubic crystals.

When referred to principal axes, the thermal expansion coefficient in an arbitrary direction is

$$\alpha_{11}' = \alpha_{11}\cos^2\phi\sin^2\theta + \alpha_{22}\sin^2\phi\sin^2\theta + \alpha_{33}\cos^2\theta,$$

where θ and ϕ are the spherical coordinate angles. When all three principal coefficients are positive numbers, the resulting surface is shaped like a peanut (Fig. 11.2). For trigonal, tetragonal, and hexagonal crystals, the thermal expansion coefficient surface is

$$\alpha_{11}' = \alpha_{11}\sin^2\theta + \alpha_{33}\cos^2\theta$$

and for cubic crystals the surface is a sphere of radius $\alpha_{11}' = \alpha_{11}$.

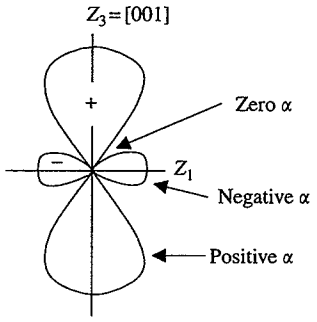

Fig. 11.3 Thermal expansion surface of calcite with circular symmetry about Z_3, the trigonal axis. The maximum expansion is perpendicular to the flat carbonate groups of the structure.

Unlike the dielectric constant, thermal expansion coefficients can be positive, negative, or both positive and negative. Trigonal calcite ($CaCO_3$) is a good example. At room temperature, the thermal expansion coefficients are $\alpha_{11} = \alpha_{22} = -5.6 \times 10^{-6}$/K and $\alpha_{33} = +25 \times 10^{-6}$/K. The resulting surface (Fig. 11.3) has both positive and negative lobes. In between the two lobes is a cone of zero thermal expansion given by $\alpha_{11}' = 0 = \alpha_{11}\sin^2\theta + \alpha_{33}\cos^2\theta$ or $\tan^2\theta = -\alpha_{33}/\alpha_{11}$. The zero expansion angle is $\theta = 65°$.

Problem 11.1

Al_2TiO_5 is orthorhombic, point group *mmm*. The structure contains chains of TiO_6 octahedra along the *c*-axis, the direction of negative thermal expansion. Measured values along the principal axes are $\alpha_{11} = 9.51$, $\alpha_{22} = 19$, $\alpha_{33} = -1.4$, all in units of 10^{-6}/K. Plot the thermal expansion as a function for direction in the (100), (010), and (001) planes. Replot this data as a quadratic surface. The large anisotropy in α leads to intergranular microfracture and low mechanical strength in aluminum titanate ceramics.

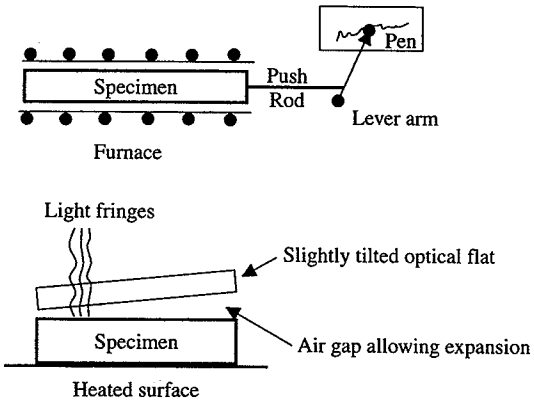

Fig. 11.4 Lever-arm dilatometers and optical interferometers are two of the experimental methods used to measure thermal expansion.

11.2 Thermal expansion measurements

Schematic illustrations of two of the classical techniques are shown in Fig. 11.4. Ceramists use push-rod dilatometers to measure the expansion of heated specimens inside a furnace. The lever arm amplifies the thermal motion. Physicists traditionally favored optical techniques. Small changes in thickness of a heated specimen were measured by counting light fringes formed by optical interference across a small air gap.

The classical techniques are sufficient for isotropic polycrystalline specimens or cubic crystals but low symmetry crystals require up to six different crystal orientations. Fortunately there is another method to measure the thermal expansion coefficients of anisotropic materials. The single crystal coefficients can all be determined from X-ray powder patterns.

The interplanar d-spacing are given by Bragg's Law

$$\lambda = 2d \sin\theta,$$

where θ is the Bragg angle and λ is the X-ray wavelength. Differentiating this equation with respect to temperature gives

$$\frac{\mathrm{d}d}{\mathrm{d}T} = -\frac{\lambda}{2}\frac{\cos\theta}{\sin^2\theta}\frac{\mathrm{d}\theta}{\mathrm{d}T}$$

from which the thermal expansion coefficient

$$\alpha_d = \frac{1}{d}\frac{\mathrm{d}d}{\mathrm{d}T} = -\cot\theta\frac{\mathrm{d}\theta}{\mathrm{d}T}.$$

The shifts in Bragg angle, $\mathrm{d}\theta/\mathrm{d}T$, are determined by recording the powder pattern at two different temperatures (Fig. 11.5).

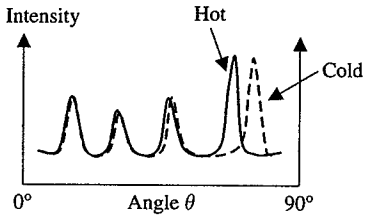

Fig. 11.5 An X-ray powder pattern recorded at two different temperatures showing the shifts in θ from which thermal expansion coefficients are calculated. The shifts are especially large in the back reflection region near 90°.

After determining the angular shifts and computing the thermal expansion coefficients for each reflection, the coefficients are plotted as a function of direction. The measured values α_d refer to the directions perpendicular to each Bragg plane (hkl). Thus for the $\bar{2}13$ reflection, the α_d value is plotted for the direction normal to $(\bar{2}13)$.

If, instead of plotting α_d, one plots $\pm 1/\sqrt{\alpha_d}$, then a representation quadric surface is obtained (see Section 9.5). A sample surface for a monoclinic crystal is shown in Fig. 11.6.

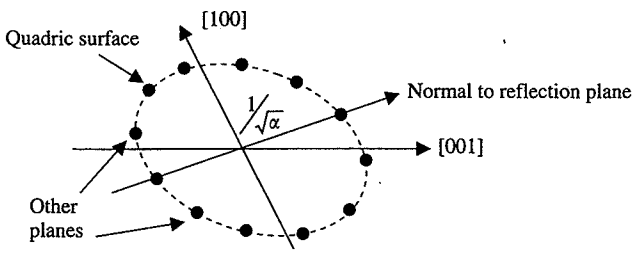

Fig. 11.6 Thermal expansion ellipsoid for a monoclinic crystal. By plotting $1/\sqrt{\alpha}$ for various planes, the principal axes can be identified.

The major and minor axes of the ellipse correspond to two of the principal axes. For a monoclinic crystal, the third principal axis is along the [010] direction.

The volume expansivity β is defined as the fractional change in volume for a 1° change in temperature: $\beta = (1/V)(\mathrm{d}V/\mathrm{d}T)$. When referred to principal axes,

$$\beta = \alpha_{11} + \alpha_{22} + \alpha_{33}.$$

The temperature dependence of the density, ρ, is

$$\frac{1}{\rho}\frac{\mathrm{d}\rho}{\mathrm{d}T} = -\beta = -(\alpha_{11} + \alpha_{22} + \alpha_{33}).$$

Problem 11.2

As pointed out in Section 6.2, there is a thermodynamic relationship between the linear thermal expansion coefficient and the piezocaloric effect. A piezocaloric experiment is performed on calcite ($CaCO_3$) using two plates cut parallel and perpendicular to the threefold symmetry axis. From the values of α_{11} and α_{33} listed in Table 11.1, calculate the changes in entropy and temperature when the plates are subjected to a compressive stress of 1000 N/m^2. Use the Law of Dulong and Petit in estimating the specific heat. The density of calcite is 2.71 g/cm^3.

11.3 Structure–property relations

Strong interatomic forces are associated with low thermal expansion, weak forces with high expansion (Fig. 11.7). The room temperature thermal expansion coefficients of cubic inorganic crystals illustrates the trend. Fig. 11.8 shows the thermal expansion coefficients of six compounds with univalent and divalent ions. In every case the divalent compounds have stronger bonds and smaller expansivities. The product of the charges differs by a factor of four and so do the thermal expansion coefficients.

Megaw has shown that α is inversely proportional to the Pauling bond strength, defined as the cation valence divided by its coordination number. For cubic ZrO_2 the Zr–O bond strength is $4/8 = 0.5$. Fig. 11.8 shows the thermal expansion coefficients plotted against bond strength. The bond strength is approximately proportional to $\alpha^{-1/2}$.

Although α depends mainly on bond strength, there are variations among isomorphous crystals. Thermal expansion coefficients for alkali halides with the

Table 11.1 Thermal expansion coefficients near room temperature in units of 10^{-6}/K

Cubic crystals	α		
Diamond (C)	1.4		
Silicon (Si)	4.2		
Germanium (Ge)	5.9		
Copper (Cu)	17		
Silver (Ag)	20		
Gold (Au)	15		
Iron (Fe)	12		
Platinum (Pt)	8.3		
Tungsten (W)	4.3		
Hexagonal crystals	α_{11}	α_{33}	
Magnesium (Mg)	27	28	
Zinc (Zn)	14	61	
Cadmium (Cd)	19	48	
Magnesium Hydroxide ($Mg(OH)_2$)	11	45	
Tetragonal crystals	α_{11}	α_{33}	
Tin (Sn)	46	22	
Titanium Oxide (TiO_2)	7.1	9.2	
Trigonal crystals	α_{11}	α_{33}	
Calcium Carbonate ($CaCO_3$)	−3.8	21	
Sodium Nitrate ($NaNO_3$)	11	120	
Tellurium (Te)	28	−1.7	
Antimony (Sb)	8.2	16	
Aluminum Oxide (Al_2O_3)	5.4	6.6	
Orthorhombic crystals	α_{11}	α_{22}	α_{33}
Iodine (I_2)	133	95	35
Lead Chloride ($PbCl_2$)	34	39	17

rocksalt structure range from NaF 34×10^{-6}/K to LiI 56×10^{-6}/K. Radius-ratio appears to be important since α is largest for LiI, LiBr, LiCl, NaI, and NaBr where r_+/r_- is small. Anion–anion repulsion loosens the structure making expansion easier.

Thermal expansion of layer-type crystals is largest normal to the layer. In hydrocarbons and other planar molecular crystals, expansion coefficients for crystalline benzene (−193°C to 3°C) are 11.9, 10.6, and 22.1 $\times$ 10^{-5}/K parallel to the *a*, *b*, and *c* orthorhombic axes. The C_6H_6 molecules in benzene lie close to the (001) plane, perpendicular to the direction of largest expansion. The same is true of naphthalene ($C_{10}H_8$) and anthracene ($C_{14}H_{10}$). Expansion coefficients are greater for crystals with small molecules than their larger homologs. The average α values for benzene, naphthalene, and anthracene are 14.7, 12.7, and 8.0×10^{-5}/K. Because of the weak bonding between molecules, the thermal expansion coefficient of organic crystals are an order of magnitude larger than those of metals and ceramics.

Anisotropy in inorganic crystals follow similar trends. Calcite is an ionic crystal consisting Ca^{2+} cations and $(CO_3)^{2-}$ anions. The flat triangular carbonate groups are perpendicular to the trigonal *c*-axis, the direction of maximum

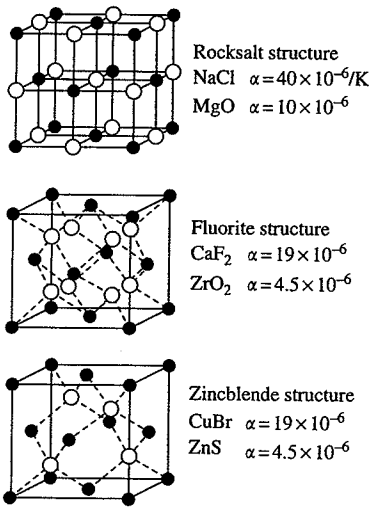

Fig. 11.7 For simple ionic structures like rocksalt and fluorite, higher valence compounds have lower thermal expansion coefficients.

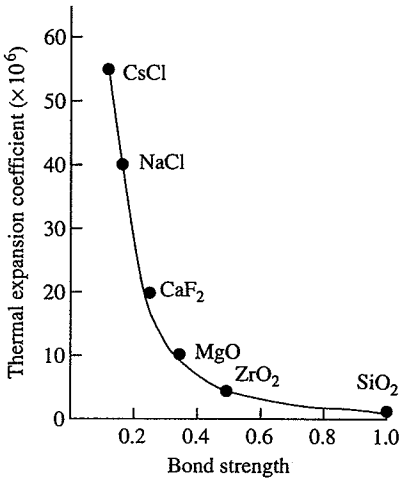

Fig. 11.8 Thermal expansion coefficients are inversely proportional to Pauling bond strength.

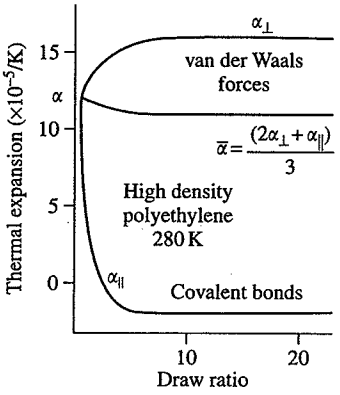

Fig. 11.9 Thermal expansion coefficients of polyethylene fibers measured parallel and perpendicular to the draw axis. As the $(CH_2)_n$ chains align under stress, the bonding and thermal expansion becomes very anisotropic.

thermal expansion (Fig. 11.3). Table 11.1 lists thermal expansion coefficients for a number of isotropic and anisotropic crystals.

Layer structures like antimony, brucite ($Mg(OH)_2$), and graphite also have the largest thermal expansion coefficients α_{33} perpendicular to the layers. Tellurium and tin have strong bonding along the c-axis making $\alpha_{11} > \alpha_{33}$. Metals also show similar anisotropy effects. Metallic zinc has a distorted hexagonal close-packed structure with the shortest bonds in the (001) plane. The thermal expansion coefficient in the perpendicular direction α_{33} is much greater than α_{11}.

Thermal expansion depends on the strength of the chemical bonds in different directions. Polymers form very long molecules with covalent bonds in the chain direction and van der Waals forces in the perpendicular directions between adjacent chains. A large anisotropy in thermal expansion is therefore expected. X-ray measurements on crystalline polyethylene along the orthorhombic axes gave $\alpha_a = 20 \times 10^{-5}/\text{K}$, $\alpha_b = 6.4 \times 10^{-5}$, and $\alpha_c = -1.3 \times 10^{-5}$. The negative value α_c along the chain axis is somewhat surprising but has been verified in other polymers. Thermal agitation gives rise to lateral vibrations in the chain which produce an effective contraction by bending motions.

In an isotropic polymer the chains are entangled in random directions, so that thermal expansion is controlled by the weak bonds between chains. When drawn into fibers, however, the polymer becomes anisotropic with a large decrease in α parallel to the fiber axis and modest increase in the perpendicular directions (Fig. 11.9).

Thermal expansion anisotropy leads to problems in polycrystalline ceramics and metals. Under thermal cycling, neighboring grains expand differently, leading to stresses at the grain boundaries. Ceramics made of cubic materials do not experience this problem because grains expand and contract uniformly as temperature changes. To relieve the intergranular stresses in anisotropic materials, it is sometimes possible to choose a composition that is accidentally isotropic. Consider the trigonal $Al_{2-x}Cr_xO_3$ grains in a ruby ceramic. The physical properties of a solid solution change smoothly from one end member to the other. In the Al_2O_3–Cr_2O_3 solid solution the thermal expansion coefficients

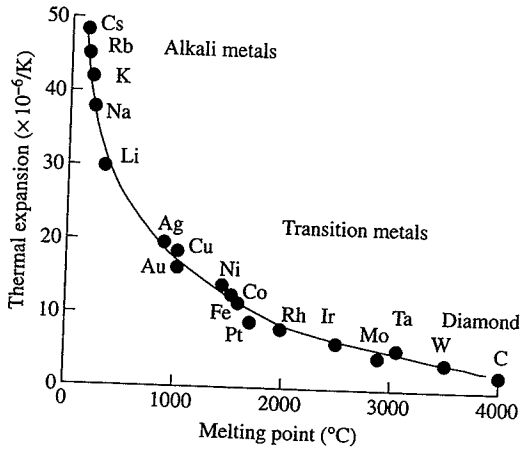

Fig. 11.10 Melting points and room temperature thermal expansion coefficients for a number of different chemical elements.

change from a positive ($\alpha_{33} > \alpha_{11}$) to a negative ($\alpha_{33} < \alpha_{11}$) anisotropy. In between there is an isotropic composition where $\alpha_{33} = \alpha_{11}$ and the intergranular stresses are minimized. This is an interesting bit of tensor engineering that improves thermal shock resistance.

11.4 Temperature dependence

There is an inverse relationship between thermal expansion and melting point, as shown in Fig. 11.10. The product αT_m is approximately constant. Low melting elements like the alkali metals have much larger coefficients than the refractory transition metal elements.

The crystal structures of MgO, BeO, Al_2O_3, $MgAl_2O_4$, and $BeAl_2O_4$ are all based on close-packed oxygen lattices and all exhibit fairly large thermal expansion coefficients, $5–10 \times 10^{-6}$/K. The effect of temperature is to increase thermal vibration, and in close-packed structures this results in atoms vibrating against one another since they are in close contact. The situation is more complicated in open structures where two additional effects can occur. The atoms can vibrate anisotropically toward open spaces in the structure, resulting in low thermal expansion coefficients. Thus many open structure oxides have small thermal expansion coefficients; compounds like spodumene (2×10^{-6}/K) are therefore useful because of their thermal shock resistance. Second, there can be cooperative rotational effects that lead to a rapid change in thermal expansion coefficients with temperature, as in quartz. The small expansivity of silica glass ($<10^{-6}$/K) has been attributed to the fact that the densities are low and also that cooperative rotations are not possible in amorphous materials.

Thermal expansion coefficients often change dramatically with temperature, especially when phase transformations are involved. The correlation between thermal expansion and melting points has already been mentioned. Refractory compounds like silica glass have small thermal expansion coefficients but the crystalline forms of silica (cristobalite, tridymite, and quartz) all have displacive phase transformations that can lead to thermal shock in silica refractories. Silica ceramics must be heated or cooled slowly below 600°C where the transitions

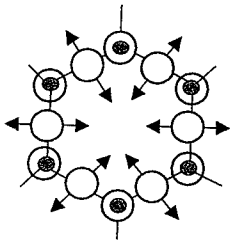

Fig. 11.11 Silica rings consist of tetrahedrally coordinated silicon atoms linked together by oxygens. Open spaces in the silicate structures leads to transverse motions of the oxygen atom causing large displacive phase transformations and unusual thermal expansion effects.

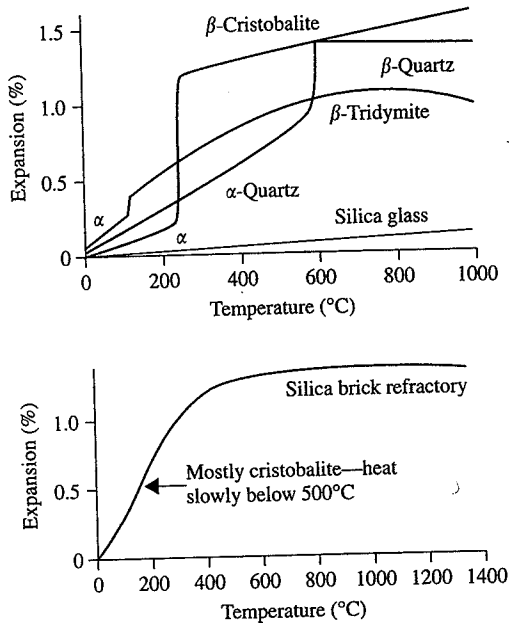

Fig. 11.12 Thermal expansion of various forms of silica and silica brick.

occur. At higher temperatures the crystalline phases have small α values similar to silica glass and the silica bricks are more resistant to thermal shock. The rapid increase in volume at the phase α–β phase transformations can be understood as an opening up of the silicate rings. At room temperature the rings (Fig. 11.11) are partially crumpled but the increase in thermal motion straightens out the silicate rings. The transverse vibrations of oxygen also explain the peculiar behavior at very low temperatures. Silica has a negative thermal expansion coefficient near 0 K because the lowest energy vibration modes are the transverse motions of the oxygen atoms. This leads to a crumpling of the silicate rings and thermal shrinkage. Zinc oxide (Fig. 11.1) shows a similar effect.

Problem 11.3

Using the data for silica brick refractories in Figure 11.12, estimate the thermal expansion coefficient α as a function of temperature from 100°C to 1400°C. Express the dependence of α on T as a power series in ΔT, $(\Delta T)^2$, $(\Delta T)^3$, etc., and derive a set of coefficients which fit the measured values of α over this temperature range.